15th October 2025. Vol.103. No.19
© Little Lion Scientific



ISSN: 1992-8645 www.jatit.org E-ISSN: 1817-3195

AN IMPLEMENTATION OF ENHANCED INCEPTION-RESIDUAL CONVOLUTIONAL NEURAL NETWORK IN LUNG CANCER PREDICTION

Dr.S.PANDIKUMAR¹, Dr.S.PREMKUMAR², Dr.T.GUHAN³, 4. T.MARGARET MARY⁴ Dr.M.KANNAN⁵, Dr.V.PREAM SUDHA⁶

¹Associate Professor, Department of MCA, Acharya Institute of Technology, Bangalore, India. ²Assistant Professor, School of Information Sciences, Presidency University, Bengaluru-560 119, India. ³Associate Professor, Department of Computer Science and Engineering,

³Akshaya College of Engineering and Technology, Coimbatore, Tamil Nadu-642 109, India. ⁴Associate Professor, Department of Computer Science, Kristu Jayanti (Deemed to be University), Bangalore.

⁵Assistant Professor & Head, Department of Computer Science, Bishop Ambrose College, Coimbatore, Tamil Nadu, India.

⁶Professor, Department of Computer Science with Data Analytics, Dr.NGP Arts and Science College, Coimbatore, Tamil Nadu, India.

ABSTRACT

Recent developments in Deep Learning are assisting in pattern recognition, classification, and quantification. Additionally, DL offers optimal performance across all industries, particularly in the medical field. For diseases to be treated and for humans to survive, precise diagnosis is essential. The primary goal of this study is to develop a useful tool for Computer Aided Diagnosis (CAD) systems to identify a suspicious lung nodule for cancer early detection automatically. Deep Learning is used to carry out this task. Using a filter, image acquisition and de-noising have been done at the first step. Segmentation and feature extraction have been accomplished in stage two. Finally, classification is accomplished using CNN methods in Deep Learning dubbed Enhanced Inception of Residual Convolutional Neural Network. Performance Evaluation metrics like accuracy, precision, recall, and f-measure are examined, and the results are also optimised. This method is contrasted with ML-E-RF and LR module 1, and it is ultimately determined that DL has a quick and precise diagnostic system.

Keywords: CT-scan, CNN, Adaptive Wiener Filter, MV-CNN, EIRCNN.

1. INTRODUCTION

Worldwide, the lung cancer is one of the leading source of death. Cilia, which are tiny hair-like structures, are present on the upper portion of the respiratory tract. These cilia assist in the removal of bacteria, dust, and other harmful substances from the lungs. When smoking, using tobacco, eating poorly, or ingesting other harmful chemicals enters the lungs and causes an infection, the cilia are destroyed, which results in lung cancer.

The human anatomy can be visualised using a variety of medical modalities. The research associated to medical image processing has the capability to comprehended quantitative characteristics of cancerous tumours for both phenotypes and genotypes and advanced our understanding of how to diagnose cancer.

Medical imaging is a non-invasive method of creating internal body parts that can be used by doctors for explorations in clinical diagnostics.

A significant count of research has been conducted through medical pictures for automated lung nodule classification, response evaluation, and treatment planning. Hover, one significant problem with human lungs is the length of time it takes to find their abnormalities, which lowers survival rates after evaluation. Only when LCs are identified in their earliest phases can a suitable therapeutic solution be found [1]. One of the most difficult yet rewarding applications of IMTs in the field of medicine is information discovery [2]. IMTs have the potential to explore and find hidden patterns from healthcare images, so they can be

15th October 2025. Vol.103. No.19

© Little Lion Scientific

www.jatit.org



E-ISSN: 1817-3195

applied to images produced by different medical imaging modalities to visualise abnormalities in the images. (3). IMTs can be used in clinical diagnostics to create precise classifier models and thereby forecast severe human diseases. In these instances, the treatments have been successful and the patients have lived. the methods and algorithms used in image mining to find LCs in CTS, X-ray, MRI, and ultrasound images that were captured with the right imaging equipment. The patient's medical pictures are

collected and entered into image processing tools

(IPTs), where they involve various process like enhancement, segmentation, feature extraction

and detection. The steps of medical image

mining for LC diagnostics are depicted in Figure

ISSN: 1992-8645

The deadliest and most frequently caused illness in the human body, cancer, has a very high causality rate. Both among males and women, LCs are the leading cause of cancer deaths. LCs produce aberrant cells that proliferate and form lesions or tumours. These cancerous cells use the blood and lymph fluids that encircle lung tissues to spread from the lungs to other organs. (4). Lung carcinoma and a healthy lung are contrasted in Figure 1.

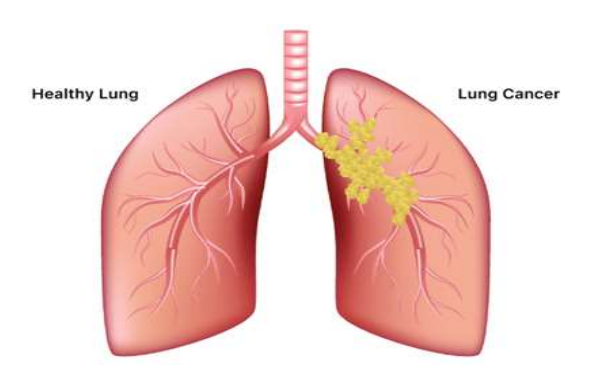


Figure 1. Healthy Lung vs Lung Cancer

Based on lymph flow, cancerous cell growths tend to gravitate towards the centre of the thorax. Metastasis is the medical term for the spread of these cells to different human systems. Despite having more treatment choices for cancer, such as surgery, radiotherapy, or chemotherapy, their mortality rates are higher, but when the disease is caught early, the survival rate can reach up to 55% over a five-year period. Therefore, it is essential to diagnose LCs early in order to stop its development andspread within the body of the patient, which will lower mortality rates. IMTs

on CTSs have been used as a potential diagnostic technique with accurate outcomes for LC detections. As lung nodules are typically benign, CTSs have become a routine medical procedure for LC assessment and detection. (5). Hard lumps are typically cancerous, despite the fact that lesions caused by calcification, swelling, and hardness may also be handled as benign lesions. (malignant). CTSs are required by radiologists for their conclusions and can aid in defining the different kinds of lesions.

A. Stages and Types of Lungs Cancer

LCs are usually grouped into two primary types: NSCLCs (non-small cell lung cancers) and SCLCs (small cell lung cancers). (Non-Small Cell Lung Cancers). Nearly 90% of LCs contain NSCLCs, with SCLCs making up the remainder. NSCLCs advance and expand gradually. SCLCs, which spread quickly, typically impact people who have a smoking habit. Depending on the spread or degree of the diagnosed LC, NSCLCs may be treated with surgery, chemotherapy, or radiotherapy. Chemotherapy is the main treatment option for SCLCs.

B.Significance of Lung CTS Images

CTSs are selected for LCs detection for a variability of factors [6]. Compared to other imaging techniques, they are the most frequently used in medicine. The large air content of human lungs prevents imaging techniques like ultrasound from successfully capturing lung images. While PET (Positron Emission Tomography) scans are used to identify advanced stages of LCs, MRI scans are very expensive. Additionally, CTSs can visualize internal bodily structures like bones, soft tissues, and blood vessels, from which three-dimensional slices can be cut out for analysis.

C. Importance of Lung X-Ray Images

X-rays are another popular imaging modality used in the detection of pulmonary diseases, much like CTSs. X-rays are common and widely used because of their modest radiation output, negligible to non-existent side effects, affordable price, and average sensitivity levels. Radiologists with expertise use X-rays to make precise calculations based on the X-ray image quality (12). When detected early, the vast majority of human illnesses are curable. Patient

15th October 2025. Vol.103. No.19

© Little Lion Scientific



ISSN: 1992-8645 www.iatit.org E-ISSN: 1817-3195

screening can be helpful in this regard [12], and the most common imaging technology is conventional chest radiography. Automations can accurately identify lung boundaries and categorise lungs with pathologies as normal orabnormal when used for X-ray-based diagnostics.

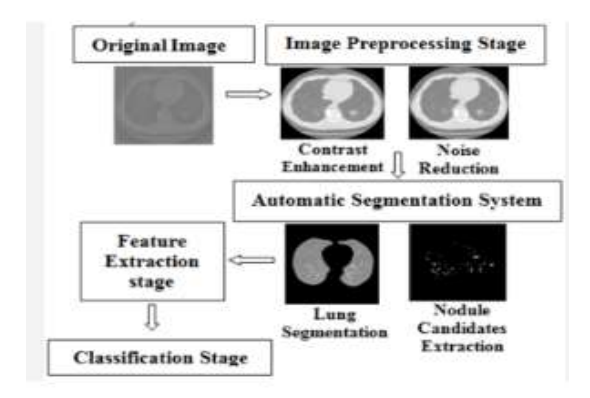


Figure 2. Schematic Diagram of CAD with Lung **Images**

2. LITERATURE REVIEW

[20], In this research, a technique for applying the Wiener filter on images that contain unknown amounts of Gaussian noise is suggested. In contradiction to the way of usual application, the variation of noise is expected by evaluating the depth intensity distribution of relatively homogeneous areas from the image and then passing that information as an input argument to the Wiener filter. In addition to it, there exists numerous research on the exploration of the influence on quality of processed photos due to this approach's filter mask size. With reference to the Wiener filter's initial implementation, encouraging results are gathered. According to CheolheeYooa, Daehyeon Han, et al., the Local Climate Zone classification system provides standardized framework to demonstrate urban functions and forms which is particularly valuable for the studies on urban heat islands To classify Landsat-based resolution LCZ maps by deploying a random forest (RF) machine learning classification algorithm the World Urban Database and Portal Tool (WUDAPT) technique has been used. In some research, the convolutional neural network (CNN) and modified RF are also recommended. This current study would undergo in-depth

comparative analysis of RF classifier and CNN for LCZ mapping are the main objective of the study. Using different combinations of input features from bitmap Landsat 8 data over four major worldwide cities: Rome, Hong Kong, Madrid, and Chicago, five schemes were created-three RF-based (S1-S3) and two CNNbased (S4-S5). Among the five schemes, the CNN-based scheme with more neighborhoods had the best classification performance. By comparing the four cities to the WUDAPT process, the overall accuracy for all land cover (OA) and urban LCZ types (LCZ1-10; OAurb) increased by around 6-8% and 10-13%, respectively. An assessment of transferability of the LCZ models for the four cities demonstrated that CNN consistently outperformed RF in terms of accuracy. Based on this study's findings, the CNN classifier performed well especially for LCZ-specific classes where buildings were mixed with plants or trees or the buildings were widely dispersed. Future deep learning-based LCZ classification can be guided by the study outcomes.

[1], In this research, the human body can be visualized using a variety of medical methods. Due to its ability to offer information on quantitative characteristics of malignant tumours for both pheno- and genotypes, medical image mining research has significantly advanced our understanding of how to diagnose cancer. Medical imaging is a non-invasive method for creating inside body components that can be used by clinicians for explorations in clinical diagnosis. For automated lung nodule categorization, response evaluation, and therapy planning, a great deal of research has been done on medical imaging. However, one significant problem with human lungs is the length of time it takes to find their defects, which lowers survival rates following diagnosis. Only when LCs are discovered in their earliest stages can a suitable therapeutic approach be developed.

[12], In this study after identifying the cotton or mists in the thorax-examined clinical images, the term "lung nodule" or "pulmonary nodule" refers to a white area. Effective diagnosis and treatment of lung illness depend on the early detection of lung nodules during thoracic computed tomography (CT) scans. Prior to that, the clustering is completed using an EWRCNN (Entropy Weighted Residual Convolution Neural Network) to identify lung nodules. This identification strategy is less dependent on scale

15th October 2025. Vol.103. No.19
© Little Lion Scientific



ISSN: 1992-8645 www.jatit.org E-ISSN: 1817-3195

and can keep a strategic distance from rival extraction. Anyhow, the differentiation of suspected aspiratory nodules necessitates additional creative effort that can increase the recognition affectability of detection systems. The enhanced inception-residual convolutional neural network (EIRCNN) has three phases such as segmentation, and classification of the pulmonary nodule—suggested to achieve this goal. Initially, the Normalized Gamma-Corrected Contrast-Limited Adaptive Histogram Equalization (NGCCLAHE)- Discrete Wavelet Transform (DWT), which allows combination of the DWT and NGCCLAHE, is advised to enhance the local information of the CT picture. Secondly, the Gray Level Feature Extraction and Fuzzy Continuous Wavelet Transform (FCWT) are deployed to direct the feature extraction from processed tomography images, and the intelligent W-Net (iW-Net) is recognized as an advanced deep learning model that integrates both automated and intuitive segmentation of lung nodules, using Gray Level Co-occurrence Matrix (GLCM) features. Then, in order to limit the immateriality and to produce an efficient set of capabilities of the feature selection remove the filter-based method. The approach EIRCNN is far more successful in lowering the false positive rates on 888 readings of the publicly accessible LIDC-IDRI dataset than other approaches like RCNN, Faster RCNN, and EWRCNN.

[3], One of the most difficult yet rewarding applications of IMTs in the field of medicine is knowledge discovery. IMTs have the potential to investigate and uncover hidden patterns from healthcare images, therefore they can be used over images produced by different medical imaging modalities to visualise anomalies in the images.

3. METHODS

This section provided an explanation of the study article's methodology. The ways in which the data sets and features were obtained are explained. The algorithms used in this research and their evaluation standards are also covered in this section.

4. DATASET DESCRIPTION

For experimental analysis, this study used public LIDC-IDRI (Lung Image Database Consortium and Image Database Resource Initiative) [14] as primary data. Each and every nodule in this collection was annotated by up to four boardcertified radiologists. In this study, only used the nodules that havecomments from all four radiologists. (a total of 750 nodules). In order to produce a single truth boundary, a 50% consensuscriterion [15] is chosen due to the variation among the four different radiologists. 143 nodules have been retained out of the total 893 nodules that were collected because they were normal images, and the remaining 750 nodules were divided into training, testing, and validation sets, respectively, to conduct a thorough evaluation of this technique.

5. MOTIVATION AND JUSTIFICATION

The major aim of this research is to detect automatic suspicious lung nodule in the image within less time. In the existing work the automatic detection is done using Machine Learning Techniques known as Enhanced-Random Forest and Linear Regression. Even though, it gives satisfactory result but it fails to detect artifacts area in the image. Therefore, this study further replies to deep learning techniques Enhanced Inception-Residual such as Convolutional Neural Network. Rapid advancements in deep learning have improved performance across industries, many particularlythe medical sector. Numerous studies supported this with evidences.

6. OBJECTIVES OF THE RESEARCH

Emerging infectious illnesses are becoming more prevalent today and harming people. The second most common illness to cause death is cancer. Developing a practical tool for Computer Aided Diagnosis (CAD) systems that would enable the early, automated identification and categorization of lung nodules is the main objective of the proposed research. The suggested methodology's specific goal is: to enhance the accuracy of the classification of pulmonary nodules in CT images.

In the Existing work some of the artifact regions are not taken in to an account. In this proposed work it is consider, so

15th October 2025. Vol.103. No.19

www.jatit.org

© Little Lion Scientific



E-ISSN: 1817-3195

image restoration method carried for better result.

- > The high false positive rate is decreased by using adaptive wiener filter techniques to help radiologists interpret images and make accurate diagnoses by differentiating between lung nodules and background tissues.
- An architectural framework known as Enhanced Inception-Residual Convolutional Neural Network was built utilizing Deep Learning Neural Network methods to automatically extract features and classify lung nodules as normal or abnormal.

7. RESEARCH CONTRIBUTIONS

ISSN: 1992-8645

Inception is a powerful neural network architecture that has been used drastically in recent eras for several processes such as natural language processing, deep learning, and image recognition. In this blog post, we will introduce an enhancement to the Inception architecture known as Enhanced Inception residual (EIR), which is designed to improve performance on certain problems. First, let's briefly describe the Inception architecture. The basic idea is to use a few very deep layers of nonlinear units, followed by a final layer of linear units, that enable to identify high-level features of the data when decreasing the data amount which should be processed.

8. DATASET

The chest LIDC/IDBC dataset can successfully be used by the proposed research methodology to identify lung nodules and predict the nodule stage. Three stages performed in this research. Stage 1 for image enhancement, segmentation, feature extraction, and finally classification to accomplish the objective of lung cancer diagnosis.

- > Utilizing a Residual Convolutional it Neural Network. effectively distinguishes between nodules and nonnodules, enhancing both precision and recall to a very high degree.
- Our approach effectively extracts characteristics from tissues and blood vessels in scan pictures while

minimizing false positives. Attained a classification accuracy of 95% at a minimum duration of 2.10 seconds.

A. Lung Cancer Detection Using Deep Learning **Techniques**

Improving data quality is the main goal of image enhancements. Denoising with filters like mean, median, Laplacian, and Gaussian filters; expanding image edges with unsharp masking or wavelet transforms; and boosting image contrast with histogram equalisations are some of the techniques used for these improvements. It can be challenging for humans to perceive and comprehend a CTS's restrictedcontrast between normal and malignant regions.

B. Pre-processing

For image restoration, we suggest a brand-new multi-patch adaptive Wiener filter algorithm in this article. A powerful new element of AWF in [9] is the incorporation of multiple patches for each pixel estimate. We use a sliding window, just like other patch-based algorithms. The reference patch is represented by the current observation window at each location. We find the patches that are most comparable to the reference patch in a specific search for the reference.

The Adaptive Wiener Filter method [8] operates on digital images, successfully attenuating White Gaussian Noise (AWGN) as per the following expression:

$$j(i,j) = m + l2 - \sigma 2 / / / (I(i,j) - m),$$

Let I represent the intensity of a pixel located in the i-th row and j-th column of the input picture, J denotes the intensity of a pixel in the output image, and σ^2 – signifies the variance of the noise contained in the input image [7]. The average brightness, or the local mean from the mask κ of the filter measuring P x Q pixels, is represented by m and is defined as

 $m = 1 \sum_{i,j \in HI(i,j)} (2)$ The variance l is found from:

$$l2 = 1 \sum_{i,j \in H} l2(i,j) - m2.$$
 (3)

If σ 2 is unknown, the filter computes the mean of local variances over all places of the mask. This is substantial.

15th October 2025. Vol.103. No.19

© Little Lion Scientific

www.jatit.org



E-ISSN: 1817-3195

ISSN: 1992-8645

Examining the principles of the Wiener filter from both a computational perspective and in terms of the quality of the filtered pictures. The equation presented proposes a method to

The noise variance of an unknown picture may be calculated using the approach proposed by Liu et al. [10]. The following equation in vector form holds for an image's specified square area when the noise is assumed to be additive [52]:

$$(i0, j0) = I(i0, j0) + n(i0, j0), (4)$$

$$v(vTI) = var(vTI0) + \sigma^2$$
, (5)

surmount this constraint.

where var means variance estimation

$$\sigma^2 = \lambda mi(KI)$$
 (6)

Determining the covariance matrix of the gradient map [53] from each evaluated area facilitates the identification of sufficiently flat areas within the noisy image based on intensity variation [10]. Subsequently, the eigenvectors and eigenvalues are calculated, and the largest eigenvalue is selected. The area is considered flat, and the average noise variance is assessed whether it is below a predefined threshold obtained via iterative testing

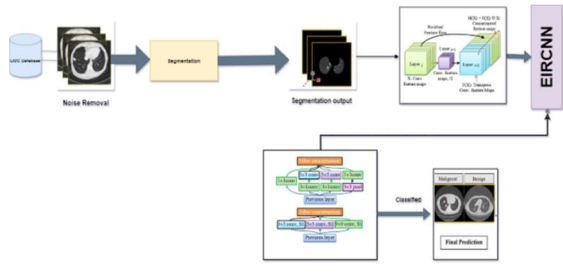


Figure 3. Architecture for Lung Cancer Detection Using Deep Learning Techniques EIRCNN

C. Segmentation

Segmentation, the second step of image processing, separates the lung regions from medical chest images so that objects and boundaries, such as lines and curves, can be detected [11]. Dividing a digital image into clusters or groupings of pixels is referred to as segmentation (segments). Another way to describe image segmentations is as the process of labelling each image pixel based on visual commonalities. We present a multi-view convolutional neural network (MV-CNN) for the segmentation of lung nodules. The MV-CNN

excelled in the simultaneous acquisition of a wide array of nodule-sensitive characteristics from axial, coronal, and sagittal viewpoints in CT images. The public LIDC-IDRI dataset's 893 nodules were used to assess the proposed method. Three branches of the proposed MV-CNN analyse the voxel patches from the axial, coronal, and sagittal view CT images, respectively. Each of the three branches has an identical architecture, consisting of a fully connected layer, two max-pooling layers, and six convolutional layers (C1 to C6). Each CNN branch of six convolutional layers is organized into three blocks. Each block has the same structure, including two convolutional layers with a kernel size of 3. Maximum pooling action with a pooling window is two between each block.

The two scale patches measure 65 X 65 and 35 X 35, respectively, and are resized to 35 X 35 with third-order spline interpolation to create a two-channel patch. The small patch has an intricate texture

$$pk = \exp(ok) / \sum_{h=\{0,1\}}^{n} \exp(oh) x^{k} a^{n-k}$$
(7)

In this context, k = 0 denotes non-nodule voxels, whereas k = 1 signifies nodule voxels. The objective of network training is to optimize the likelihood of an accurate class. This is accomplished by reducing the cross-entropy loss for each training instance. Let y represent the true label for a certain input patch that belongs to the set $\{0, 1\}$; the loss function is defined accordingly.

D. Feature Extraction

In this research, the feature is extracted using a fractal model. The dimensions have been minimized, and the most relevant characteristics that may effectively distinguish the different classes have been determined by feature selection to address the issue of high input features [17]. In order to extract eigenvalues from the image and decrease the dimension, the fractal algorithm has been implemented with the aid of covarianceanalysis. The raw images for the fractal algorithm must be of uniform dimensions. An image is referred to as a two-

15th October 2025. Vol.103. No.19
© Little Lion Scientific



ISSN: 1992-8645 www.jatit.org E-ISSN: 1817-3195

dimensional matrix and a singular vector. Images must be in greyscale and conform to certain size specifications. By reformulating matrices, each image is converted into a column vector, and the pictures are derived from a matrix of dimensions M x N, where N represents the number of pixels per image and M is the total number of images.

To ascertain the standard deviation of the average image from each original image, the average image must be calculated. The covariance matrix is calculated, followed by the of determination its eigenvalues eigenvectors. The fractal algorithm's approach is to provide M, the overall count of instructional images, Fi, their average, and li, each image inside the Ti vector. To ascertain the standard deviation of the average image from each original image, the average image must be calculated. The covariance matrix is calculated, followed by the determination of its eigenvalues and eigenvectors. The fractal algorithm's approach is to provide M, the overall count of instructional images, Fi, their average, and li, each image inside the Ti vector.

Initially, there are M pictures, each with dimensions N × N. Each picture may be represented in an N-dimensional space as determined by Equation (1), while averaging procedures are defined by Equation (2) [16].

$$A = N \times N \times M$$

(8)

$$Fi = \frac{1}{M} Tt(9)$$

Calculating the standard deviation is a crucial aspect of the fractal process, determined by Eq. (3) and the covariance matrix, where A = [Variance1, Variance2, ..., Variance] and $Cov = N2 \times N2$, with $A = N2 \times M$. Consequently, Cov is significantly elevated. The eigenvalues of the covariance matrix have now been derived.

 S_T = $(x_k$ - $\mu)(x_k$ - $\mu)T(10)$ WFractal= argmax $W^T S_T W = w_1 w_2 ... wf$ where μ represents the mean of all samples and wi for i = 1, 2, ..., f constitutes a set that identifies the item initially with only minor modifications to the image.

E. Enhanced Inception-Residual Convolutional Neural Network for Lung Nodule Detection (EIRCNN)

The Enhanced Inception-Residual Convolutional Neural Network (EIRCNN), a

variant of Deep Convolutional Neural Networks (DCNN), leverages the capabilities of Recurrent Convolutional Neural Networks (RCNN), Inception architectures, and Residual frameworks. This method enhances the accuracy of the Inception-remaining system's acknowledgment while maintaining the same amount of system parameters. The Inception network, RCNN, and Residual network get markedly enhanced training accuracy due to their innovative architecture [12].

Inception-v422,23 is currently required for the use of inception-residual units. It is organised using a deep learning model that links the beginning segment's measured convolution kernels to the results of the convolution tasks. An improved version of Inception-v3 that incorporates a large origin component and lower order channels is called Initiation-v4.

Furthermore, Inception-v4 has a residual network architecture for the inception network, referred to as the Inception-v4 Residual Network, which often improves the precision of recognition assignments. The yields of the initiation blocks are combined with the individual blocks' contributions in the Inception-Residual method.

The image indicates that the overall model comprises many convolutional layers, EIRCNN squares, transition blocks, and a Softmax function at the output unit.

The EIRCNN layer, including RCLs, inception layers, and residual layers, is the main focus of this work. After passing through inception units where RCLs were imposed, the sources that were provided for the information layer were finally combined with the contributions of the IRCNN-square.

The genesis layer's recurrent convolution operations operate on the kernels of various dimensions. The convolution unit's internal recurrent structure causes the results of the current time step to be combined with those of the previous time step.

The outputs from the current time step serve as inputs for the subsequent time step. Comparable responsibilities were executed concerning the

15th October 2025. Vol.103. No.19
© Little Lion Scientific



ISSN: 1992-8645 www.jatit.org E-ISSN: 1817-3195

evaluated time intervals.

This is a mere aggregation of feature maps about the time steps, without any alteration in the size of the IRCNN segment, input, or output. Consequently, the more beneficial attributes guarantee enhanced recognition accuracy with the same number of system parameters. The RCL's functions are completed concerning the discrete time intervals sent by the RCNN [14]. Let us examine the xl input test in the lth layer of the EIRCNN-square, together with the pixel located at (i,) in the input lung images on the kth feature map (fm) inside the RCL. Furthermore, let us consider the expected output of the network Outl(t) at the time step t. Here, x(i,j)(t)and xr(i,j)(t-1) denote the inputs for the normal convolution layers and the lth.

RCL independently. The wfm and wr values represent the loads for the standard convolutional layer and the RCL of the kth feature map, respectively, while bk denotes the bias.

y = af(outl(t)) = max(0, outlijk(t))(11)In this context, af denotes the usual Rectified Linear Unit (ReLU) activation function. Similarly, examined the performance of this model using the Exponential Linear Unit (ELU) activation function in subsequent studies. The outputs γ of the original units for the unique kernels dimension and standard pooling layer are denoted as $y1\times1$ (x), $y3\times3$ (x), and $y1\times 1p$ (x) accordingly. The final the Inception output Recurrent Convolutional Neural Networks (IRCNN) unit is denoted as (xl, wl), which can be expressed as

$$(xl, wl) = yl \times l (x) \bigcirc y3 \times 3 (x) \bigcirc yl \times lp$$

 $(x)(12)$

Here ② addresses the link activity about the channel or feature map pivot. The yield of the IRCNN unit is then included via the contributions of the EIRCNN-square. The residual activity of the EIRCNN-square may be expressed by the following equation.

$$xl+1=xl+(xl,wl) \quad (13)$$

x (l+1) denotes the contributions for the

immediate subsequent transition block, xl refers to the information representation of the EIRCNN-square, wl indicates the weight parameters of the lth EIRCNN-block, and $\mathfrak{F}(xl,wl)$ represents the output from the lth layer of the IRCNN-unit.Layers are analogous to those in the EIRCNN-square. Batch normalization is applied to the outputs of the IRCNN-square. Ultimately, the yields of this EIRCNN-square are determined by the contributions of the immediate subsequent transition unit. In the transition unit, many jobs are executed alongside convolution, pooling, and dropout, depending on their placement inside the transition block of the system.

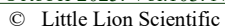
The dimensions of the input and output features are the same in the IRCNN squares; it is only a linear projection on a comparable scale, with non-linearity associated with the RELU and ELU activation functions.

In this instance, 0.5 failures after each convolutional layer inside the transition unit. Ultimately, we used a Softmax layer, or normalized exponential function, near the conclusion of the design. For the input lung sample x, weight vector W, and K unique linear functions, the Softmax operation for the ith class may be expressed as follows:

$$P(y=i/x) = e^{xT}w = e^{xT}w/\sum_{k=1}^{k} xtW_{K=1}$$
 (14)

The proposed EIRCNN architecture underwent extensive testing via several trials on diverse benchmark datasets and was evaluated against different models. For small amount of data E-RF is better, for executing larger datasets we go for DL, in ML techniques while using larger datasets the accuracy getting down so DL techniques is better for larger datasets. This analysis has been further enhanced by the Improved Stacked Autoencoder and the Enhanced Pre-Activation Residual Convolutional Neural Network. In this blog post, we will introduce an enhancement to the Inception architecture known as Enhanced Inception residual (EIR), which is designed to improve performance on certain problems. First, let's briefly describe the Inception architecture. The basic idea is to use a few very deep layers of nonlinear units, followed by a final layer of linear units, which enables to identification of

15th October 2025. Vol.103. No.19





ISSN: 1992-8645 www.jatit.org E-ISSN: 1817-3195

high-level features of the data while reducing the amount of data that needs to be processed.

Table 2: Performance Evaluation Metrics For CT (Precision)

EXPERIMENTAL ANALYSIS

The experimental results show that using classifier EIRCNN produces best classification mission. For implementing the proposed algorithm, MATLAB 2018 version software tool is used. From Lung Image Database Consortium image collection, CT images were taken, which were web-accessible international resource development, evalution and training of computer-assisted diagnostic (CAD) techniques for lung cancer detection and diagnosis. Totally 750 CT scan images are used out of 893. Using the proposed methods performance metrics like recall, precision, fmeasure, and accuracy were evaluated. Table 1 and Table 2, Table 3, Table 4 shows Performance evaluation metrics of the existing and proposed algorithm with CT images. From the below Figure. 4 to Figure .7, it can be observed that the comparison metric is evaluated.

Table 1: Performanceevaluation Metrics For CT (ACCURACY (%))

DATA SET	No. of images (Accuracy (%))	E-RF	EIRC NN
LIDC CT	150	92.25	96.23
images	300	92.34	96.15
	450	91.01	96.25
	600	90.31	97.12
	750	90.11	97.82

DATA SET	No. of images (Precision)	E-RF	EIRC NN
LIDC CT	150	79.89	83.04
images	300	81.26	83.30
	450	81.12	83.81
	600	82.01	84.25
	750	82.11	84.87

Table 3: Performance Evaluation Metrics For CT (Recall)

DATA SET	No. of images (Recall)	E-RF	EIRC NN
LIDC CT	150	95.31	97.10
images	300	95.66	97.17
,	450	95.78	97.43
	600	95.89	97.82
	750	96.11	97.96

Table 4: Performance Evaluation Metrics For CT (F-Measure)

DATA SET	No. of images (F- measure)	E-RF	EIRC NN
LIDC CT	150	88.12	92.11
images	300	88.25	92.16
	450	88.36	92.48
	600	88.88	92.88
	750	88.98	92.91

15th October 2025. Vol.103. No.19

© Little Lion Scientific

www.jatit.org



E-ISSN: 1817-3195

100 E-RF EIRCNN

75
50
25

ISSN: 1992-8645

Figure 4: Accuracy for CT

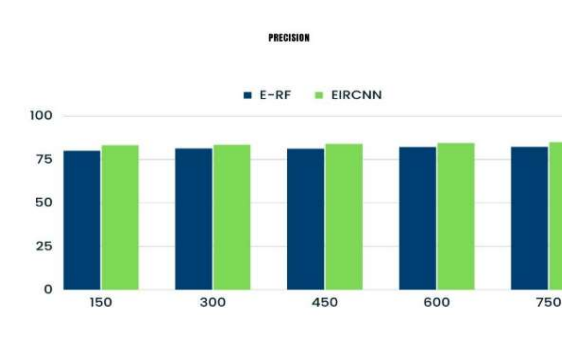


Figure 5: Precision for CT

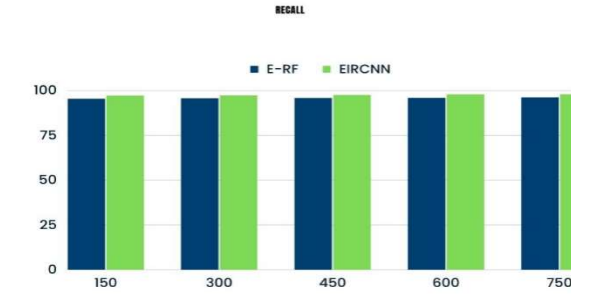


Figure 6: Recall for CT

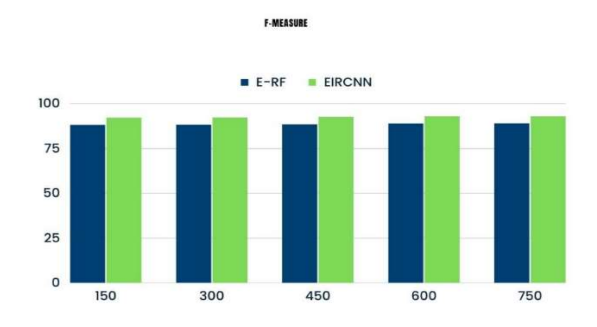


Figure 7: F-measure for CT

CONCLUSION

Inception is a robust neural network design widely used in image identification; however, an initial contrast enhancement is essential due to image processing procedures that may provide undesirable outcomes when the source images exhibit low contrast. The enhanced image displays the lung area with a crystal-clear backdrop. A lung nodule detection system for thoracic CT images is developed, driven by deep learning principles. Here, the image enhancement is performed initially using Adaptive wiener filter, segmentation is performed using Multiview convolutional neural network extraction fractal technique. Following this phase in lung nodule detection, classification is completed by the Enhanced Inception Residual Convolutional Neural Network. This detection approach might eliminate the need for candidate extraction due to less reliance on scalability. Numerous FP areas are identified in the data as E-RF and LR, independent of anatomical features. The suggested EIRCNN aims to reduce false positives, enhance algorithm accuracy, and optimize detection by accounting for various types of nodules. This analysis is further augmented by the Improved Stacked Autoencoder and the Enhanced Pre-Activation Residual Convolutional Neural Network.

REFERENCES

- [1]. Iakovidis, D.K, Schober, D, Boeker, M and Schulz, S, (2009). An ontology of image representations for medical image mining. IEEE International Conference on Information Technology and Applications in Biomedicine, pp. 1-4.
- [2]. Koczkodaj, W.W, Przelaskowski, A and Szopinski, K.T, (2010). Medical knowledge mining from image data– synthesis of medical image assessments for early stroke detection. Machine Graphics and Vision, vol. 19, no. 1, pp. 283-298.
- [3]. Wagle, S, Mangai, J.A and Kumar, V.S, (2013). An improved medical image

15th October 2025. Vol.103. No.19

© Little Lion Scientific



E-ISSN: 1817-3195

ISSN: 1992-8645 www.jatit.org

- classification model using data mining techniques. IEEE GCC Conference and Exhibition (GCC), pp. 114-118.
- [4]. Coudray, N, P.S. Ocampo, Sakellaropoulos, T, Narula, N, Snuderl, M, Fenyö, D, Moreira, A.L, Razavian, N and Tsirigos, A, (2018). Classification and mutation prediction from non-small cell lung cancer histopathology images using deep learning. Nature medicine, vol. 24, no. 10, pp.1559-1567.
- [5]. Kumar, D, Chung, A.G, Shaifee, M.J, Khalvati, F, Haider, M.A and Wong, A, (2017).Discovery radiomics for pathologically-proven computed tomography lung cancer prediction. International Conference Image Analysis and Recognition, pp. 54-62.
- [6]. Miah, M.B.A and Yousuf, M.A, (2015). Detection of lung cancer from CT image using image processing and neural network. International conference on electrical engineering and information communication technology (ICEEICT), pp. 1-6.
- [7]. Lora Petkova and Ivo Draganov, (2020). Noise Adaptive Wiener Filtering of Images, University of Durham. Downloaded on November 01,2020 at 14:43:39 UTC from IEEE Xplore.
- [8]. X. Liu, M. Tanaka, and M. Okutomi, "Noise Level Estimation using Weak Textured Patches of a Single Noisy Image", 19th IEEE International Conference on Image Processing, pp. 665-668, Orlando, FL, USA, Sept. 30 – Oct. 3, 2012.
- [9]. Armato, S. G. III, McLennan, G., Bidaut, L., McNitt-Gray, M. F., Meyer, C. R., Reeves, A. P., Zhao, B., Aberle, D. R., Henschke, C. I., Hoffman, E. A., Kazerooni, E. A., MacMahon, H., Van Beek, E. J. R., Yankelevitz, D., Biancardi, A. M., Bland, P. H., Brown, M. S., Engelmann, R. M., Laderach, G. E., ... Clarke, L. P. (2011). The Lung Image Database Consortium (LIDC) and Image Database Resource Initiative (IDRI): A completed reference database of lung nodules on CT scans. Medical Physics, 38(2), 915-931
- [10]. X. Zhu, P. Milanfar, "Automatic Parameter Selection for Denoising Algorithms using a No-reference Measure of Image Content",

- IEEE Transactions on Image Processing, vol. 19, no. 12, pp. 3116-3132, 2010.
- [11]. Ausawalaithong, W. Thirach, A, Marukatat, S and Wilaiprasitporn, Τ, (2018). November. Automatic lung cancer prediction from chest X-ray images using deep learning approach. IEEE Biomedical Engineering International Conference (BMEICON), pp. 1-5.
- [12]. K.S. Gowri Laksshmil, Dr.R. Umagandhi, An Effective Pulmonary Nodule Detection in Ct and X-Ray Images Using Enhanced Inception-Residual Convolutional Neural Network. Annals of R.S.C.B., ISSN:1583-6258, Vol. 24, Issue 2, 2020, Pages. 133 -148, Received 24 October 2020; Accepted 15 December 2020.
- [13]. Bonavita, I, Rafael-Palou, X, Ceresa, M, Piella, G, Ribas, V and Ballester, M.A.G, (2020). Integration of convolutional neural networks for pulmonary nodule malignancy assessment in a lung cancer classification pipeline. Computer methods and programs in biomedicine, pp. 1-30.
- [14]. K.S. Gowri laksshmi, R.Umagandhi, Lung Nodule Detection: Image Enhancement using Fuzzy Rule Based Contrast Limited Adaptive Histogram Equalization and Entropy Weighted Residual Convolution Neural Network Method in CTS. International Journal of Recent Technology and Engineering (IJRTE) ISSN: 2277-3878, Volume-8 Issue-4, November 2019.
- [15]. G. Armato III, G. McLennan, L. Bidaut, M. F. McNitt-Gray, C. R. Meyer, A. P. Reeves et al., "The lung image database consortium (lidc) and image database resource initiative (idri): a completed reference database of lung nodules on ct scans," Medical physics, vol. 38, no. 2, pp. 915-931, 2011.
- [16]. T. Kubota, A. K. Jerebko, M. Dewan, M. Salganicoff, and A. Krish-"Segmentation of pulmonary nodules of various densities with morphological approaches and convexity models," Medical Image Analysis, vol. 15, no. 1, pp. 133-154, 2011.
- [17]. Srinivasan A, Battacharjee P, Prasad AI, Sanyal G. Brain MR image analysis us- ing discrete wavelet transform with fractal feature analysis. In: Proceedings of the 2nd international conference on electronics,

15th October 2025. Vol.103. No.19 © Little Lion Scientific



ISSN: 1992-8645 www.jatit.org E-ISSN: 1817-3195

- communication and aerospace technology, ICECA 2018; 2018. p. 1660-4.
- [18]. Chaurasia V, Chaurasia V. Statistical feature extraction-based technique for fast fractal image compression. J Vis Commun Image Represent 2016; 41:87–95.
- [19]. K. S. Gowri Laksshmi and 2Dr. R. Umagandhi, "False Positive Reduction Based on Anatomical Characterization Using Deep Learning Neural Network In Lung Nodule Detection", European Journal of Molecular & Clinical Medicine ISSN 2515-8260 Volume 7, Issue 8, 2020.
- [20]. L. Petkova and I. Draganov, "Noise Adaptive Wiener Filtering of Images," in Proceedings of the IEEE International Conference on Image Processing (ICIP), 2020.